Thermal transport phenomena beyond the diffusive regime

P.O. Chapuis, T. Nghiem, C. Abs Da Cruz
Centre for Energy and Thermal Sciences, Lyon (CETHIL),
University of Lyon (CNRS - INSA Lyon – UCBL),
F 69621 Villeurbanne (Lyon), France
olivier.chapuis@insa-lyon.fr

E. Nefzaoui
Laboratoire Electronique, Systèmes de communication,
et Microsystèmes (ESYCOM),
ESIEE Paris, Université Paris-Est,
93162 Noisy-le-Grand, France

Abstract— **Heat conduction in semiconductors is mediated by thermally-excited phonons. When dimensions smaller than the mean free path are involved, nondiffusive heat conduction arises. In addition, surface effects related to thermal boundary resistances become significant when the dimensions of the considered media decrease. These two phenomena significantly alter thermal transport in comparison to predictions made with standard heat diffusion and result in larger temperature levels at the heat source, which can be detrimental for electronics devices. We tackle few examples where these effects are observed.**
By using the Boltzmann Transport Equation (BTE) for phonons or approximated solutions, we show that *effective cross-plane thermal conductivity reduction* takes place. We then present results of heat conduction from a metallic line of nanometer-scale width towards a flat bulk. We show that 2D ballistic heat conduction takes place and that a *ballistic reduction factor* associated to the phonon rarefaction effect should be included. The dissipated heat fluxes are reduced in comparison to the Fourier prediction. The consequence is that strong hot spots may arise. We then analyze the effect of surface imperfect transmission in thermal boundary resistance and introduce a method based on acoustics to compute it. We show that confinement and imperfect transmission lead to similar reduction of the effective thermal conductivity.

***Keywords*—heat conduction; thermal phonon; thermal boundary resistance; ballistic transport; Boltzmann transport equation.**

I. INTRODUCTION

Heat conduction is known since the XIXth century and the work by Fourier [1]. It states that the local heat flux density $\vec{q}$ is proportional to the temperature gradient through a quantity termed thermal conductivity *k*:

$$\vec{q} = -k.\vec{\nabla}T\,. \tag{I.1}$$

Applying Fourier's diffusion law requires in principle the continuity of the temperature field so that it can be locally derived. At perfect interfaces between two media, the most usual conditions are continuity of the flux, which arises from energy conservation, and continuity of temperature. This second condition is not necessarily kept as such when the interface is not ideal: voids or third bodies can be present at the mechanical contact between two solids. Most of the current simulation tools rely on the heat equation derived from Fourier's law:

$$\rho c_p \frac{\partial T}{\partial t} = \nabla(k\nabla T) + \dot{q}\,, \tag{I.2}$$

where ρc_p is the heat capacity per unit volume and $\dot{q}$ is the heat source/bath per unit volume. It is well known that the heat equation suffers from various deficiencies. As an example, the flux transferred across a film of thickness *L* writes

$$q = k\frac{\Delta T}{L}, \tag{I.3}$$

which diverges when *L* becomes arbitrarily small. Since the flux should stay finite, either the temperature difference vanishes or there is a physical length where the diffusive regime cannot be applied anymore.

A first typical length is the mean free path Λ, which is the average distance that an energy carrier travels between two scattering events [2]. In semiconductors, phonons, i.e. collective vibrations of atoms, are these carriers. At room temperature or higher, phonons can be considered as quasiparticles, provided that the size of the medium is larger than 5 nm. As a result, the phonon mean free path is of paramount importance in modern nanoelectronic devices, which routinely involves sub-micrometric sizes. The 14 nm node of the ITRS was reached in the last years [3], which means that sub-50 nm features are ubiquitous in devices and components.

A second typical length is the one where the right hand side of Eq. (I.3) is comparable to the thermal boundary conductances (TBC) per unit surface g_i (i=1,2) at the boundaries of the film. Indeed, the heat flowing across the film has also to cross its boundaries, and even in the case of perfect contact the heat transmission is not perfect. In a macroscopic way the total thermal resistance associated to Eq. (I.3) writes

$$\frac{\Delta T}{q} = \frac{1}{g_1} + \frac{L}{k} + \frac{1}{g_2}, \qquad \text{(I.4)}$$

which shows that the TBCs can indeed be neglected for large thicknesses, but that it is not possible for small L.

Other deficiencies of the heat equation could be mentioned [2], especially in the transient domain. For instance, when more than one type of energy carriers coexist in a medium, non-equilibrium between them is possible, leading to more than one local temperature. In addition, it has been observed since the 1950s that Fourier's law is instantaneous, which is not possible in reality due to constraints associated with the velocity of light [4-5].

In the following, we restrict ourselves to thermal transport in the stationary regime. We will successively observe the effects of the ballistic regime ($L < \Lambda$) of energy transport in 1D and in 2D, and of phonon transmission coefficients at boundaries.

II. BALLISTIC THERMAL TRANSPORT IN 1D

In this section, we analyze the effect of confinement within a thin layer and its effect on heat dissipation in one-dimensional configurations across such layer close to room temperature. The average mean free path in silicon is known to be close to Λ~300 nm since the pioneering work by the Goodson group [6]. This means that films of similar thickness cannot be simulated within the diffusive regime with usual Finite Element Method-based tools.

A. Computing the local non-equilibrium temperature

The key dimensionless number used to define the transition between the diffusive (Fourier) regime and the ballistic regime is the Knudsen number which compares the medium size L to the mean free path:

$$Kn = \frac{\Lambda}{L} \cdot \qquad \text{(II.1)}$$

In both the diffusive (Kn < 0.05) and the ballistic regimes (Kn >> 1), the phonon transfer can be simulated by solving the Boltzmann Transport Equation (BTE) under the relaxation time approximation [7]:

$$\frac{\partial n_p}{\partial t} + \vec{v}_{g,p}.\vec{\nabla} n_p = -\frac{n_p - n^o}{\Lambda_p / v_{g,p}}, \qquad \text{(II.2)}$$

where $\Lambda_p(\omega)/v_{g,p}(\omega)$ is the phonon relaxation time, v_g being the group velocity (velocity at which the energy is propagating), which depends on the frequency and the dispersion branch p (polarization). At equilibrium, the population of thermally-excited phonons is given by the Bose-Einstein distribution function $n°(\omega,T)=1/\exp(\hbar\omega/k_BT)$, where ω is the circular frequency, $\hbar$ the reduced Planck constant and k_B the Boltzmann constant. We note $n_p(\omega,\vec{r},T)$ the phonon distribution function out of equilibrium. In the stationary regime, the first term vanishes and the equation to solve is

$$\frac{dn_p}{ds} = -\frac{n_p - n^o}{\Lambda_p}, \qquad \text{(II.3)}$$

where s is the curvilinear abscissa. This shows that for large mean free paths no gradient of n can be obtained and that for small mean free paths the distribution function should stay close to equilibrium. The Knudsen number appears in this equation if it is made nondimensional (with $s = L\,s^*$, where s^* is the nondimensional curvilinear abscissa). If $\vec{u} = (\theta,\varphi)$ defines the angles of propagation direction of a phonon, the local energy per unit volume can be computed as

$$\begin{aligned} E(\vec{r}) &= \sum_p \int_0^{\omega_{\max,p}} \int_{4\pi} \hbar\omega\, n_p(\omega,\vec{u},\vec{r})\, \frac{g_p(\omega)}{4\pi} d\vec{u}\, d\omega \\ &= \sum_p \int_0^{\omega_{\max}} \int_{4\pi} \frac{I_p(\omega,\vec{u},\vec{r})}{v_{g,p}} d\vec{u}\, d\omega \end{aligned} \qquad \text{(II.4)}$$

where $g_p(\omega) = \omega^2/(2\pi^2 v_{\varphi,p}^2 v_{g,p})$ is the phonon density of states with v_φ as the phase velocity. In the following the phonon dispersion is considered isotropic and only the phonon population n can be anisotropic. $d\vec{u} = d\theta \sin\theta\, d\varphi$ and I is the phonon spectral radiance [8], similar to the photon one used in thermal radiation. The sum in Eq. (II.4) is over the three polarizations (see Fig. 1: two transverse acoustic modes TA and one longitudinal acoustic mode LA - we remind that the contribution of the LO+TO optical modes to heat conduction is neglected due to their low group velocity $v_g = d\omega/dk$). In contrast to photons, phonon frequency is limited by a maximal value $\omega_{\max}$.

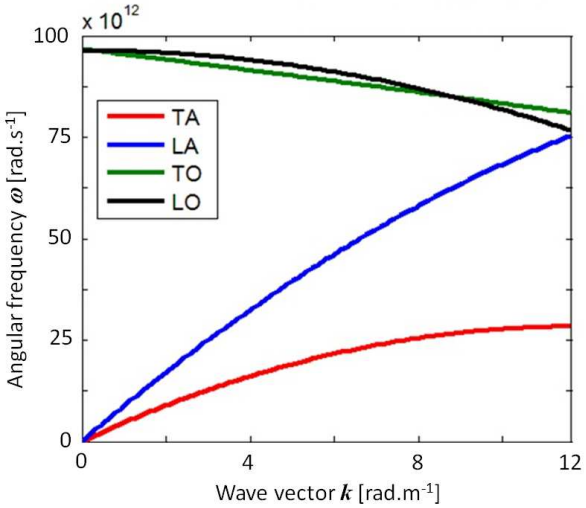

Fig. 1. Dispersion curves of silicon along the [100] (ΓX) direction in a quadratic approximation [2]. $k=\omega/v_\varphi$ is the wavevector. Note that silicon is often considered as isotropic.

The local temperature $T(\vec{r})$ can be computed by determining the equilibrium temperature that would provide the same local energy:

$$\sum_p \int_0^\infty \int_{4\pi} \frac{I^o(\omega,\vec{u},T(\vec{r}))}{v_{g,p}} d\vec{u}\, d\omega = E(\vec{r}), \qquad \text{(II.5)}$$

where I^o is obtained from n^o. It is important to understand that this local temperature is not a quantity acceptable in usual thermodynamics which requires at least the so-called local thermodynamic equilibrium (L.T.E.), i.e. that the distribution function be close to that of equilibrium n^o and weakly anisotropic [9]. The local temperature is sometimes termed as an 'effective' or 'kinetic' temperature.

If $T \ll \hbar\omega_{\max} / k_B$, the velocity of a dispersion branch can be considered as constant with $v_{\varphi,p} = v_{g,p}$: this is the Debye approximation. If verified for all dispersion branches, the local temperature is computed from

$$4\sigma_{phn} T(\vec{r})^4 = \sum_p \int_0^\infty \int_{4\pi} I_p(\omega,\vec{u},\vec{r})\, d\vec{u}\, d\omega \cdot \qquad \text{(II.6)}$$

where $\sigma_{phn} = \frac{\pi^2}{60} \frac{k_B^4}{\hbar^3 v^2}$ is the Stefan-Boltzmann constant for phonons. The Equation of Phonon Radiative Transfer (EPRT) [8] considers a Debye approximation and that $\omega_{\max} \to \infty$. The previously-mentioned condition on temperature is not met around room temperature in crystalline solids: $k_B T / \hbar \sim 40$ THz, while for silicon Fig. 1 shows that highest contributing frequency is $\omega_{\max} \sim 75$ THz. However, the EPRT allows introducing all the key concepts associated to the ballistic regime in a qualitative manner by avoiding unnecessary complexity due to atomic dispersion and frequency cut-off. In the following, we will present results from full BTE solutions or from the EPRT. The following results have been obtained with the Discrete Ordinate Method (DOM) [10] in the two cases.

B. Local temperature distribution

Fig. 2 shows the temperature profile for the ideal case of a layer sandwiched between two surfaces with perfect transmission (no reflection) respectively at 300.5 K and 299.5 K. In Fig. 2a, single-mean free path is considered, and it is possible to provide a Knudsen number. It can be seen that the well-known linear and continuous profile of the diffusive regime flattens and leads to temperature discontinuities at the boundaries when the medium size decreases (i.e. when *Kn* increases). In reality, the mean free paths of phonons depend on their frequency and a distribution of mean free paths should be accounted for [11]. For silicon, Fig. 2b shows that submicrometric films depart already from the continuous linear diffusive profile. In contrast to the ideal single (gray) mean free path case, the profiles cannot be assimilated to lines. The average mean free path in silicon is estimated to be close to 300 nm [6].

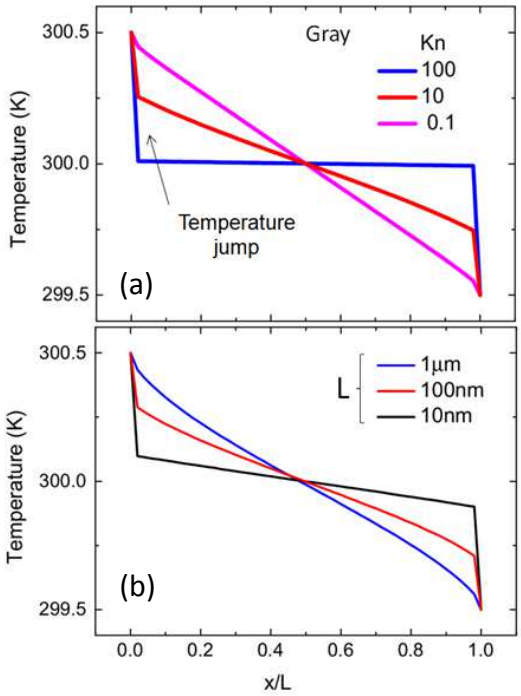

Fig. 2. Temperature profile in a film sandwich between perfect boundaries: (a) case of a single mean free path; (b) case of a distribution of mean free paths.

C. Impact on the heat flux

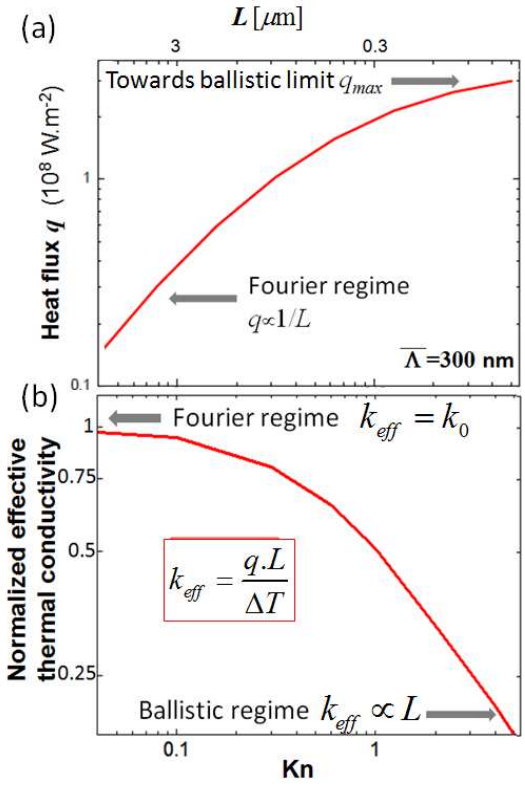

Fig. 3. Heat flux and thermal conductivity computed within the EPRT frame as a function of the layer thickness for a sinlge mean free path of 300 nm. (a) Heat flux; (b) effective cross-plane thermal conductivity.

Fig. 3 shows that reducing the thickness (i.e. increasing *Kn*) leads to increasing the heat flux. A leveling-off can be observed for thicknesses much lower than the mean free path, while an inaccurate application of Fourier law (Eq. (I.3)) predicts a diverging $1/L$ behavior. The consequence is that the ballistic regime sets a maximum heat flux that can be transferred. Eq. (I.3) can be kept as valid but the thermal conductivity should then be considered as size-dependent: $k(L)$. In this case a reduction takes place for thin films (see Fig. 3b). For a film of 60 nm the single mean free path approximation in the EPRT frame predicts an effective thermal conductivity reduced by more than 80% in comparison to the bulk.

Here, we have shown that the *cross-plane thermal conductivity* is strongly reduced. We underline that the in-plane thermal conductivity is also reduced [12].

III. BALLISTIC THERMAL TRANSPORT IN 2D

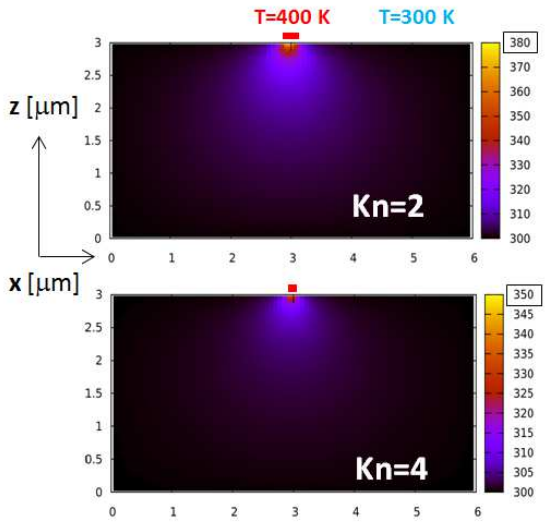

Fig. 4. Local temperature distributions for two different *Kn* related to the heat source size.

We now turn to the bi-dimensional geometry in Cartesian coordinates [13-14]. We consider an electrically-conducting wire deposited on top of a substrate. This situation is usual in components and devices, and remembers also the geometry used in the 3ω method allowing for the determination of thermal conductivity of nanomaterials [15]. The wire, heated through Joule effect, is considered as a source of fixed temperature at the boundary of the computational domain of area $L_x L_z$ = 3x3 μm^2 in the *xz* plane (see Fig. 4). Translational invariance is assumed along the *y* direction. The key dimension is now the width of the line heat source *w*. As a result, we define the Knudsen number as $Kn=\Lambda/w$. In the simulations, the wire temperature is set at 400 K, while the other boundaries are set at 300 K. The results are obtained within the EPRT frame considering again an average mean free math of 300 nm. It is again seen that a temperature jump takes place close to the source: maximal temperatures in the domain reach respectively 380 K and 350 K for *Kn* = 2 and *Kn* = 4, in contrast to 400 K predicted with Fourier's law. Similarly to the 1D case, this means that heat dissipation is less efficient. Note that this effect has been called 'phonon rarefaction' by analogy with the 'rarefied gas regime' known at reduced pressure in vacuum chambers.

The implementation of adiabatic conditions at the boundaries in contact with the source would lead to situation closer to realistic situations. In this case, the thermal resistance associated to heat dissipation between the wire and a flat surface (considering no boundaries along *x* direction) is known to be [16]

$$R_{th} = \frac{A + \ln(\frac{2L_z}{w})}{\pi L_y k}. \qquad \text{(IV.1)}$$

if L_y is the transverse length of the metallic wire. A = 1.048417 is a numerical constant close to $\int_0^{\pi/2} \frac{\tanh u \, \sin^2 u}{u^3} \, du$. In this case, it would be shown that *Kn* and the mean free path Λ would take part in the expression and increase the resistance. The effect can be embedded in a geometry-dependent thermal boundary resistance, which could enable the use of usual FEM simulations with effective parameters. Alternatively, a *ballistic reduction factor* can be defined. We note that accounting for the real shape of the wire would possibly lead also to nonequilibrium issues [17-18]. Thermal boundary resistance at the wire-substrate interface should also be considered in this case.

In both the 1D and the 2D cases, heat dissipation is reduced. This often leads to increased local temperature and may be detrimental in many devices and components.

IV. THERMAL BOUNDARY RESISTANCES

We now turn to the analysis of the transmission of phonons at boundaries between two materials. Phonons can be considered as acoustic waves as in continuum elasticity theory if their wavelength is not too small, i.e. if the variation of their group velocity stays close to the sound velocity – then atomic acoustic dispersion can be neglected. It is the case for low-frequency phonons (with frequencies lower than few THz). One can easily understand that the probability for a phonon travelling into a first medium to be transmitted toward a second medium will depend on the acoustic impedances of the two media. The problem is similar to an optical wave being partly reflected at an interface, where the quantity of energy transmitted depends on the well-known Fresnel coefficients [2].

The key information associated to the thermal boundary resistance is the ability for a phonon to be transmitted across the interface. The coefficient of transmission in energy from medium A to medium B is noted $\tau(\omega,\theta)$, and depends both on the frequency and the angle of incidence. The flux transferred *q* [W.m^{-2}] is therefore [2]

$$q = \sum_{P} \iiint_{\theta\in[0,\pi/2],\varphi\in[0,2\pi]} \hbar\omega(k)\left(n_A^o(k).v_{g,A}(\vec{k}).\cos\theta.\tau_{A\to B}(\vec{k}) - n_B^o(k).v_{g,B}(\vec{k}).\cos\theta.\tau_{B\to A}(\vec{k})\right)\frac{dk\,kd\theta\sin\theta d\varphi}{(2\pi)^3} \quad \text{(II.1)}$$

where (θ,φ) are the angles defining the direction of propagation of a phonon before impinging the surface between media A and B. The sum is performed over the polarizations *p*, i.e. for one longitudinal and two transverse waves. The thermal conductance *G* [W.m^{-2}.K^{-1}] across the boundary is given by the derivative of the flux with respect to temperature, i.e.

$$G = \sum_{P} \iiint_{\theta\in[0,\pi/2],\varphi\in[0,2\pi]} \hbar\omega(k)\left(\frac{dn_A^o}{dT}(k).v_{g,A}(\vec{k}).\cos\theta.\tau_{A\to B}(\vec{k}) - \frac{dn_B^o}{dT}(k).v_{g,B}(\vec{k}).\cos\theta.\tau_{B\to A}(\vec{k})\right)\frac{dk\,kd\theta\sin\theta d\varphi}{(2\pi)^3} \quad \text{(II.2)}$$

with the thermal resistance [K.m^2.W^{-1}] being the inverse.

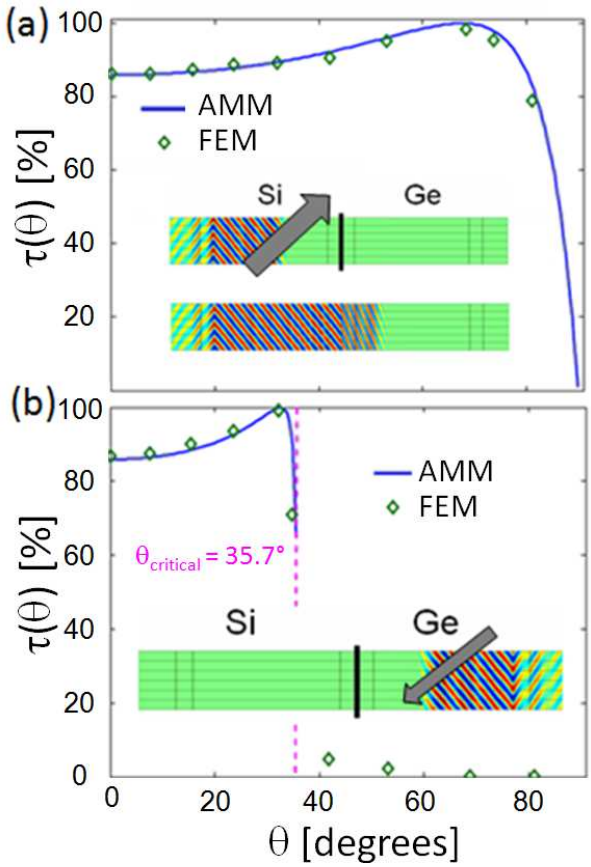

Fig. 5. Transmission coefficients across a Si→Ge (a) or Ge→ Si (b) interface as a function of the angle of incidence in the longitudinal case.

While thermal resistance can readily be calculated from molecular dynamics simulation at equilibrium or out of equilibrium directly [19], this frame allows determining precisely which modes are transferred and which ones are reflected. In the purely acoustic framework, there is no frequency dependence for perfectly flat interfaces. The calculation of the thermal conductance can be done analytically for the flat interface and is known as the Acoustic Mismatch Model (AMM) [20]. However, the phonon wavelengths (up to few nanometers) at room temperature are of similar order to that of atomic lattice constants or natural roughness for electronics materials such as silicon, and the reflection at interfaces is generally diffuse and not specular as considered in the AMM.

We have developed a tool based on acoustics (linear elasticity) to compute the transmission coefficients [21]. Such tool is in principle valid only at low temperature and we aim at comparing the predictions around room temperature or higher with results accounting for atomic acoustic (phonon) dispersion (see Fig. 1). These results can be obtained within the lattice dynamics framework, which considers that matter is discrete. In our tool, we excite acoustic plane waves and send them toward an interface for a set of frequencies and angles. We compute the energy reflected at the interface, therefore determining the transmission coefficient. The computational domain is periodic in the direction perpendicular to the interface. Absorbing conditions are set close to the source and symmetrically at the opposite side (see Fig. 5) [21].

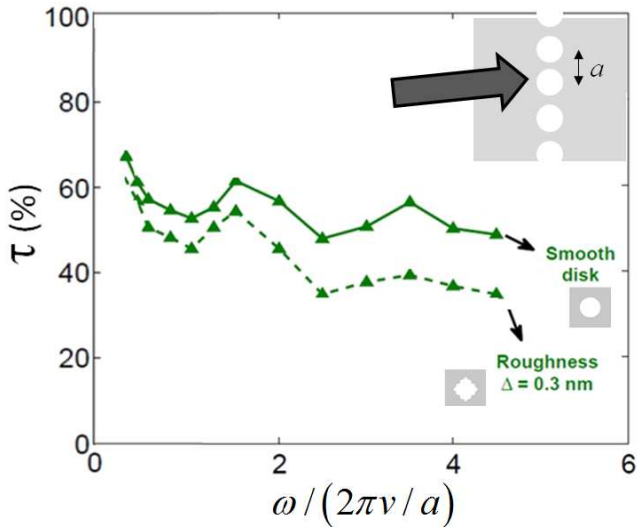

Fig. 6. Transmission coefficients across an array of scatterers with circular shape or corrugated circular shape, as a function of nondimensional frequency.

The interest of this tool is its ability to allow designing arbitrary shapes at the interface, provided some periodicity perpendicularly to the interface can be set. It is particularly suitable for computing the transmission coefficients of rough interfaces or situations involving objects scattering phonons. In order to show its powerfulness, we have analyzed in 2D the case of a periodic array of circular objects (see Fig. 6) – the period of the array is a = 100 nm and the radius of a hole is $R = a/4$ - and the transmission is integrated over all incidence angles. Circular holes or corrugated holes have been considered and showed that corrugations can reduce the transmission of phonons through such periodic arrays. Note

that the corrugations, built here from 8 small disks at the limits of a hole, deviate by up to $R/6$ from the ideal circular shape. The computations from this acoustic method should be compared with results of the Diffuse Mismatch Model (DMM) [22] currently used to determine the thermal resistance across interfaces close to room temperature. We underline that DMM also suffers from lacks [23-24]. In particular, it cannot tackle the case of close-to-identical materials in contact. Real acoustic simulations embedding roughness are therefore preferable.

V. CONCLUDING REMARKS

We have shown that for a thin film two mechanisms can block the heat dissipation: non-perfect transmission at interfaces (wave effect) and particle confinement. While the two have been treated separately here for pedagogical purpose, they should be combined in real cases. Indeed, it is not possible to add simply the effects by attributing a thermal resistance to each of them. As a result, a full frequency-dependent treatment involving the BTE should be implemented, with the transmission coefficient calculated with the method described in Section IV.

We note that we have not considered the electron-phonon interaction in confined media [25] and the related transient issues [26]. This can be done by solving simultaneously the BTE for phonon and electrons in the time domain [27].

ACKNOWLEDGMENTS

We acknowledge the support of EU project FP7-LARGE QuantiHeat, of project INSA BQR MaNaTherm, and of the French Research Agency ANR through project RPDOC NanoHeat. We also acknowledge discussions with many colleagues within the frame of GDR Thermal Nanosciences and Nanoengineering.

REFERENCES

[1] J. Fourier, Theorie Analytique de la Chaleur, Paris: Firmin Didot, 1822.

[2] P.-O. Chapuis, Introduction to heat transfer at nanoscale, Chap. 3, pp. 39-81, in "Thermometry at the nanoscale: Techniques and selected applications", F. Palacios and L. Carlos ed., RSC Publishing: London, 2015.

[3] International Technology Roadmap on Semiconductors. See http://www.itrs2.net

[4] C. Cattaneo, "Sur une forme de l'équation de la chaleur éliminant le paradoxe d'une propagation instantanée", Comptes Rendus de l'Académie des Sciences (Série I), vol. 247, p. 432, 1958.

[5] P. Vernotte, "Les paradoxes de la théorie continue de l'équation de la chaleur", Comptes Rendus de l'Académie des Sciences, vol. 246, p. 3154, 1958.

[6] M. Asheghi, Y.K. Leung, S.S.Wong, and K. Goodson, "Phonon-boundary scattering in silicon thin films", Appl. Phys. Lett., vol. 71, p. 1798, 1997.

[7] P.G. Klemens, "The Thermal Conductivity of Dielectric Solids at Low Temperature (Theoretical)", Proc. Roy. Soc. Lond. A, vol. 208, pp. 108-133, 1951.

[8] A. Majumdar, "Microscale heat conduction in dielectric thin films", J. Heat Transfer, vol. 115, p. 7, 1993.

[9] G. Chen, Nanoscale Energy Transport and Conversion: A Parallel Treatment of Electrons, Molecules, Phonons, and Photons, MIT-Pappalardo Series in Mechanical Engineering ed.: Oxford, 2005.

[10] B.G. Carlson and K.D. Lathrop, "Transport theory: the method of discrete ordinates", in H. Greenspan, C.N. Kelber, D. Okrents, Computing methods in reactor physics, Gordon and Breach: New York, 1968.

[11] A.S. Henry and G. Chen, "Spectral Phonon Transport Properties of Silicon Based on Molecular Dynamics Simulations and Lattice Dynamics", J. Comput. Theo. Nanosci., vol. 5, pp. 1-12, 2008.

[12] E. Chávez-Ángel, J.S. Reparaz, J. Gomis-Bresco, M.R. Wagner, J. Cuffe, B. Graczykowski, A. Shchepetov, H. Jiang, M. Prunnila, J. Ahopelto, F. Alzina, and C.M. Sotomayor Torres, "Reduction of the thermal conductivity in free-standing silicon nano-membranes investigated by non-invasive Raman thermometry", APL Materials, vol. 2, 012113, 2014.

[13] R.G. Yang, G. Chen, M. Laroche, and Y. Taur, "Simulation of Nanoscale Multidimensional Transient Heat Conduction Problems using Ballistic-Diffusive Equations and Phonon Boltzmann Equation", Journal of Heat Transfer, vol. 127, pp. 298-306, 2005.

[14] A. Mittal and S. Mazumder, "Generalized Ballistic-Diffusive Formulation and Hybrid SN-PN Solution of the Boltzmann Transport Equation for Phonons for Nonequilibrium Heat", vol.133, 092402, 2011.

[15] D.G. Cahill, "Thermal conductivity measurement from 30 to 750 K: The 3ω method", Review of scientific instruments, vol. 61, p. 802, 1990.

[16] M. M. Yovanovich, Y. S. Muzychka, and J. R. Culham, "Spreading Resistance of Isoflux Rectangles and Strips on Compound Flux Channels", J. Thermophys. Heat Transf., vol. 13, pp. 495-500, 1999.

[17] S. Volz and P.-O. Chapuis, "Increase of Thermal Resistance Between a Nanostructure and a Surface due to Phonon Multireflections", J. Appl. Phys., vol. 103, 034306, 2008.

[18] P.-O. Chapuis, M. Prunnila, A. Shchepetov, L. Schneider, S. Laakso, J. Ahopelto, and C.M. Sotomayor Torres, "Effect of phonon confinement on heat dissipation in ridges", Proceedings of THERMINIC 16 (Thermal Investigation of ICs and Systems), Barcelona (Spain), October 6th-8th, 2010.

[19] E. S. Landry and A. J. H. McGaughey, "Thermal boundary resistance predictions from molecular dynamics simulations and theoretical calculations", Phys. Rev. B, vol. 80, 165304, 2009.

[20] I.M. Khalatnikov, "An introduction to the theory of superfluidity", Zh. Eksp. i Teor. Fiz., vol. 22, p. 687, 1952.

[21] T. Nghiem and P.-O. Chapuis, "Phononic thermal resistance due to a finite periodic array of nano-scatterers", submitted (2016).

[22] E.T. Swartz and R.O. Pohl, "Thermal Boundary Resistance", Reviews of Modern Physics,,vol. 61, p. 605, 1989.

[23] S. Merabia and K. Termentzidis, "Thermal boundary conductance across rough interfaces probed by molecular dynamics", Phys. Rev. B, vol. 89, 054309, 2014.

[24] H.-K. Lyeo and D.G. Cahill, "Thermal conductance of interfaces between highly dissimilar materials", Phys. Rev. B, vol. 73, p. 144301, 2006

[25] S. Sinha, E. Pop, R. W. Dutton, and K. E. Goodson, "Non-Equilibrium Phonon Distributions in Sub-100 nm Silicon Transistors," ASME Journal of Heat Transfer, 128, pp. 638-647, 2006.

[26] A. Arbouet, N. Del Fatti, F. Vallée, M. Pellarin, and M. Pileni, "Electron-Phonon Scattering in Metal Clusters", Phys.Rev. Lett., vol. 90, p. 177401, 2003.

[27] T.T.T. Nghiem, J. Saint-Martin, and P. Dolfuss, "Electro-thermal simulation based on coupled Boltzmann transport equations for electrons and phonons", J. Comput. Electron., vol. 15, pp. 3-15, 2016.